

Nov 13th

Simplified Design Approach for Laterally Braced Purlins Subjected to Wind Uplift

Roger A. LaBoube

Missouri University of Science and Technology, laboube@mst.edu

Follow this and additional works at: <https://scholarsmine.mst.edu/isccss>



Part of the [Structural Engineering Commons](#)

Recommended Citation

LaBoube, Roger A., "Simplified Design Approach for Laterally Braced Purlins Subjected to Wind Uplift" (1984). *International Specialty Conference on Cold-Formed Steel Structures*. 2.

<https://scholarsmine.mst.edu/isccss/7iccfss/7iccfss-session1/2>

This Article - Conference proceedings is brought to you for free and open access by Scholars' Mine. It has been accepted for inclusion in International Specialty Conference on Cold-Formed Steel Structures by an authorized administrator of Scholars' Mine. This work is protected by U. S. Copyright Law. Unauthorized use including reproduction for redistribution requires the permission of the copyright holder. For more information, please contact scholarsmine@mst.edu.

SIMPLIFIED DESIGN APPROACH FOR Laterally Braced
PURLINS SUBJECTED TO WIND UPLIFT

by

Roger A. LaBoube¹

Introduction

Cold-formed C- or Z-sections are used extensively by the metal building industry as secondary roof framing members - commonly called purlins. In this application, one flange of the purlin is attached to a roof panel. This flange functions as the tension flange of the purlin when the roof system is subjected to a wind uplift load. The compression flange is often restrained from lateral movement by intermediate braces located at either the mid-point or third-points along the span of the purlin.

A series of simulated wind uplift load tests were conducted, in order to gain insight into the ultimate load carrying capacity, for C- and Z-purlins laterally braced at discrete locations along the compression flange. This paper describes the test program, presents a simplified design procedure and discusses the correlation between the tested and computed ultimate load capacity.

Literature Review

For a doubly symmetric I-beam, the critical stress for elastic lateral-torsional buckling is given by the following well known equation(7):

$$f_{cr} = \frac{C_b \pi}{S_x L} \sqrt{EI_y GJ \left(1 + \frac{\pi^2 EC_w}{GJ L^2} \right)} \quad (1)$$

All parameters are defined in Appendix II.

As discussed in Ref. 7, by applying the appropriate geometric relationships and recognizing that the St. Venant torsional rigidity can be neglected, Eq. 1 can be simplified as follows:

$$f_{cr} = \frac{C_b \pi^2 E d I_{yc}}{L^2 S_{xc}} \quad (2)$$

¹Research Engineer, Butler Manufacturing Company - Research Center, Grandview, Mo.

To predict the critical inelastic lateral-torsional buckling stress, a parabolic transition curve is used. This curve, as discussed by Yu⁽⁷⁾, is described by the following formula:

$$f_{cri} = F_y \left(1.11 - \frac{1}{3.24} \frac{F_y (L^2 S_{xc}/d I_{yc})}{C_b \pi^2 E} \right) \quad (3)$$

Although Eqs. 2 and 3 were developed for I-shaped sections, Hill⁽²⁾ indicated that these equations can also be applied to C-shaped sections. On this basis, Ref. 1 provides that the design stress, for symmetrical C-shaped sections bending about the centroidal axis perpendicular to the web, be limited by either Eq. 4 or Eq. 5 for elastic and inelastic buckling, respectively:

$$F_b = 0.6 \pi^2 E C_b \frac{d I_{yc}}{L^2 S_{xc}} \quad (4)$$

$$F_b = \frac{2}{3} F_y - \frac{F_y^2}{5.4 \pi^2 E C_b} \left(\frac{L^2 S_{xc}}{d I_{yc}} \right) \quad (5)$$

Reference 6 reveals, that for Z-shaped sections, a seemingly conservative approach was adopted. The allowable stress, for beams governed by elastic buckling, was taken as one-half of that given by Eq. 4

$$F_b = 0.3 \pi^2 E C_b \frac{d I_{yc}}{L^2 S_{xc}} \quad (6)$$

For Z-sections governed by inelastic buckling, the following transition formula is employed:

$$F_b = \frac{2}{3} F_y - \frac{F_y^2}{2.7 \pi^2 E C_b} \left(\frac{L^2 S_{xc}}{d I_{yc}} \right) \quad (7)$$

The appropriate limits for elastic versus inelastic buckling are given in Ref. 1.

Experimental Study

A total of eight specimens were tested. These specimens had compression flange braces at either the mid-point or third-point along the span. Table 1 gives a summary of the test program.

Each test specimen consisted of two 20 ft. (15.2 m) long purlins having cross-section dimensions as listed in Table 2. The purlins were spaced 5 ft. (1.5 m) apart, which is consistent with typical metal building construction practice. The tension flange of each purlin was affixed to a conventional roof panel by using self-drilling screws on 12 in. (305 mm) centers. The test specimen was mounted, in an inverted position, in a vacuum test chamber. Figure 2 is a schematic of the test setup. Figures 3 and 4 show the overall test setup. A detailed discussion of the test setup is presented in Reference 4.

The simulated wind uplift load was applied by evacuating air from beneath the test specimen. A pressure transducer was used to measure the applied load. Both the horizontal and vertical deflections of the compression flange were measured by linear transducers. The measurements were recorded at 5 psf, 15.8 lb/ft (230 N/m), increments until failure.

The braces used in the test program were steel tubes having a 1 in. (25.4 mm) nominal diameter and a 0.06 in. (1.5 mm) wall thickness. The tubes were strain gaged and calibrated in a Tinius Olsen testing machine. To prevent introducing bending in the tubes, and to facilitate making vertical adjustments during the test, the purlin to tube connection was made by using a ball and socket mechanism (Figure 5). Figure 6 shows the screw jack which was used to maintain the horizontal position of the braces during the test. The strain gage readings were also recorded at loading increments of 15.8 lb/ft (230 N/m). A discussion of the measured brace forces is given in Ref. 5.

Evaluation of Test Results

An analysis was performed to evaluate the ability of Eqs. 4 through 6 to estimate the capacity of the Z- and C-purlins used in the test program. To obtain the computed failure load, the appropriate value of F_b (from Eqs. 4 through 6), is amplified by a factor of 1.67, which is the implied factor of safety. Summarized in Table 3 for each test specimen, is the tested ultimate load, P_u , the computed ultimate load, P_1 and the corresponding ratio of P_u/P_1 .

The magnitude of the ratio P_u/P_1 provides an indication of the accuracy of the analytical model. For the Z-sections (Specimens No. 5 through 8), this ratio ranges from 0.91 to 0.95, which demonstrates that Eq. 7 yields a reasonable numerical value for the allowable bending stress of a laterally unbraced Z-purlin.

For the C-purlins (Specimens No. 1 through 4) the value of the ratio P_u/P_1 varied from 0.68 to 0.78. These numerical values indicate that Eq. 5 significantly over estimates the capacity of the test specimens, which is contrary to Hill's (2) findings. This poor correlation may be the result of several factors. First, Hill in his experimental study used aluminum C-sections that had stocky webs, which precluded the occurrence of web buckling and its influence on the capacity of the test specimens. Also, Hill loaded his test specimens such that the unsupported length was subjected to pure bending, whereas, the test specimens for the work presented herein, were loaded in such a manner that the unbraced length was subjected to a varying moment diagram, as depicted by Figure 7.

Modified Design Procedure

As a result of the above discussion, a modified design procedure is proposed for both Z- and C-shaped sections subjected to a wind uplift loading.

Z-Sections: To reflect the influence of local buckling of the web, on the ultimate capacity of the purlin, controlled by inelastic lateral-torsional buckling, Eq. 6 should be modified as follows:

$$F_b = \frac{2}{3} F - \frac{F^2}{2.7 \pi^2 E C_b} \left(\frac{L^2 S_{xc}}{d I_{yc}} \right) \quad (8)$$

where F is the smaller value of F_y or $1.67 F_{bw}$. The latter is given by Section 3.4.2 of Ref. 1.

By using the above equation, the computed load capacity was evaluated and is given in Table 4 as P_2 . The ratio of P_u/P_2 is also given in Table 4, and indicates a small improvement in the correlation between test and computed load capacities for the Z-purlins used in this test program.

C-Sections: Based upon a previous discussion, modifications are necessary to reflect both the web buckling implications, and also, the variation observed in the distribution of the applied moment.

The web buckling can be handled in the same manner as for the Z-shaped sections, by limiting the maximum stress to F_y or $1.67 F_{bw}$. However, the variation in the moment diagram is not as straightforward. Typically, the variation in the moment has been reflected by the value of C_b from Eq. 9 and given on Fig. 7

$$C_b = 1.75 + 1.05 \left(\frac{M_1}{M_2} \right) + 0.3 \left(\frac{M_1}{M_2} \right)^2 \quad (9)$$

Equation 9 was developed from studies which used simply supported doubly-symmetric beams⁽³⁾.

It appears that a modification in C_b would be proper for monosymmetric C-shapes, but, ill advised without a comprehensive study of the variations in the moment distributions. Therefore, the modification will be reflected not in C_b , but in the numerical constant that appears in the denominator of Eq. 8. It is proposed that the maximum compressive stress in the extreme fibers of a laterally unsupported C-purlin be limited by

$$F_b = \frac{2}{3} F - \frac{F^2}{3.5 \pi^2 E C_b} \left(\frac{L^2 S_{xc}}{d I_{yc}} \right) \quad (10)$$

Equation 10 yields computed load capacities, P_3 , as given in Table 5. Also listed in Table 5 is the corresponding ratio of P_u/P_3 for each test specimen which varied from 0.90 to 1.14.

Conclusion

Based upon test results obtained for both C- and Z-purlins subjected to a simulated wind uplift load, simplified design equations were developed. These equations provide a reasonable estimate of the capacity of a purlin, for which the failure is controlled by inelastic lateral-torsional buckling. The equations also reflect the interaction of local web buckling and overall buckling.

No data was developed for C- and Z-purlins governed by elastic lateral-torsional buckling. However, it is the author's opinion that the current equations (Eqs. 3.3-2 and 3.3-4 given in Ref. 1) should provide a reasonable estimate of the load capacity. This opinion is attributed to the fact that the overall slenderness will be of such a magnitude, that local web stability will have little, if any, influence on the member behavior. Also, the member stiffness will not be as sensitive to variations in the moment gradient - C_b should yield a reasonable estimate of the effect of moment gradient.

APPENDIX I - REFERENCES

1. American Iron and Steel Institute, "Specification for the Design of Cold-Formed Steel Structural Members," 1980 ed.
2. Hill, H. N., "Lateral Buckling of Channels and Z-Beams," ASCE Transactions, Vol. 119, 1954.
3. Johnson, B. G. (ed.), "Guide to Stability Design Criteria for Metal Structures," 3rd ed., Wiley-Interscience, New York, 1976.
4. LaBoube, R., and Thompson, M., "Static Load Tests of Braced Purlins Subjected to Uplift Load," MRI Project 7485-G, Midwest Research Institute, Kansas City, Mo., August 1982.
5. LaBoube, R. A., "Purlin Braces: Measured Forces," Proceedings, Third International Colloquium on Stability of Metal Structures, Toronto, Canada, May 1983.
6. Winter, G., "Commentary on the 1968 Edition of the Specification for the Design of Cold-Formed Steel Structural Members," American Iron and Steel Institute, 1970 ed.
7. Yu, W. W., Cold-Formed Steel Structures, McGraw-Hill Book Co., 1973.

APPENDIX II - NOTATIONS

- C_b = bending coefficient dependent upon moment gradient.
 C_w = warping constant of torsion of the cross section.
 E = modulus of elasticity of steel.
 F = maximum stress level, F_y or $1.67 F_{bw}$.
 F_b = maximum allowable compressive stress in the extreme fibers of laterally unsupported beam.
 F_{bw} = maximum allowable web compressive stress due to bending.
 F_y = yield stress.
 G = shear modulus of steel.
 I_y = moment of inertia about y axis.
 I_{yc} = moment of inertia of the compressive portion of a section about y axis.
 J = St. Venant torsion constant of the cross section.
 L = unbraced length of member.
 M_1 = smaller end moment.
 M_2 = larger end moment.
 P_u = test failure load.
 P_1 = computed failure load using Eq. 5 or 7.
 P_2 = computed failure load using Eq. 8.
 P_3 = computed failure load using Eq. 10.
 S_x = section modulus about x axis.
 S_{xc} = compression section modulus of entire section about x axis.
 d = depth of section.
 f_{cr} = elastic critical buckling stress for lateral-torsional buckling.
 f_{cri} = inelastic critical buckling stress for lateral-torsional buckling.

SEVENTH SPECIALTY CONFERENCE

TABLE 1

SUMMARY OF TEST PROGRAM

<u>Test No.</u>	<u>Section Type*</u>	<u>Brace Location</u>	<u>Span Length, SL (in.)</u>
1	C	.50 SL	237.5 ↓
2	C	.50 SL	
3	C	.33 SL	
4	C	.33 SL	
5	Z	.50 SL	
6	Z	.50 SL	
7	Z	.33 SL	
8	Z	.33 SL	

*See Figure 1

TABLE 2

CROSS SECTION DIMENSIONS

Test No.	Purlin Location	H (In.)	B1 (In.)	B2 (In.)	L1 (In.)	L2 (In.)	R1 (In.)	R2 (In.)	t (In.)	ϕ (degree)	F_y (ksi)
1	N	9.06	2.56	2.44	.81	.75	.30	.23	.078	86	61.61
	S	9.06	2.50	2.56	.81	.75	.30	.23	.079	83	62.45
2	N	9.06	2.56	2.50	.81	.75	.27	.23	.078	85	63.09
	S	9.06	2.63	2.50	.81	.75	.28	.23	.080	86	60.37
3	N	9.13	2.56	2.50	.81	.75	.30	.23	.079	85	62.93
	S	9.06	2.50	2.56	.81	.75	.27	.22	.078	82	63.85
4	N	9.06	2.56	2.44	.81	.75	.30	.23	.078	86	61.16
	S	9.06	2.50	2.56	.81	.75	.30	.23	.079	83	62.45
5	N	8.13	3.00	2.75	.81	.81	.23	.34	.087	76	55.16
	S	8.13	3.00	2.75	.75	.81	.25	.36	.087	74	55.16
6	N	8.13	3.00	2.75	.81	.81	.27	.38	.086	74	55.40
	S	8.13	2.94	2.74	.81	.81	.23	.38	.085	72	57.76
7	N	8.19	2.94	2.69	.75	.88	.30	.34	.092	74	58.00
	S	8.19	3.00	2.69	.81	.88	.28	.38	.092	76	58.00
8	N	8.19	3.00	2.69	.81	.88	.27	.34	.092	74	56.50
	S	8.19	3.00	2.69	.81	.94	.28	.34	.092	75	56.60

Note: See Figure 1 for definition of cross section notations.

SEVENTH SPECIALTY CONFERENCE

TABLE 3

EXPERIMENTAL vs. COMPUTED CAPACITY

<u>Specimen No.</u>	<u>P_u (lb/ft)</u>	<u>P₁ (lb/ft)</u>	<u>P_u/P₁</u>
1	184.4	237.9	0.78
2	171.9	235.4	0.73
3	181.3	264.9	0.68
4	187.5	259.6	0.72
5	225.0	238.8	0.94
6	215.6	230.4	0.94
7	265.6	281.0	0.95
8	259.4	284.6	0.91

Note: P_u, is the ultimate test load at failure.

P₁, is computed by using F_b x 1.67, where F_b was governed by Eq. 5 or 7, respectively.

TABLE 4

COMPARISON OF EXPERIMENTAL AND MODIFIED
COMPUTED CAPACITY FOR Z-SECTIONS

<u>Specimen No.</u>	<u>P_u (lb/ft)</u>	<u>P₂ (lb/ft)</u>	<u>P_u/P₂</u>
5	225.0	235.3	0.96
6	215.6	226.9	0.95
7	265.6	278.1	0.96
8	259.4	282.0	0.92

Note: P_u, is the ultimate test load at failure

P₂, is computed by using $F_b \times 1.67$, where F_b is given by Eq. 8.

TABLE 5

COMPARISON OF EXPERIMENTAL AND MODIFIED
COMPUTED CAPACITY FOR C-SECTIONS

<u>Specimen No.</u>	<u>P_u (lb/ft)</u>	<u>P₃ (lb/ft)</u>	<u>P_u/P₃</u>
1	184.4	166.6	1.11
2	171.9	168.3	1.02
3	181.3	202.6	0.89
4	187.5	200.3	0.94

Note: P_u, is the ultimate test load at failure

P₃, is computed by using $F_b \times 1.67$, where F_b is given by Eq. 10.

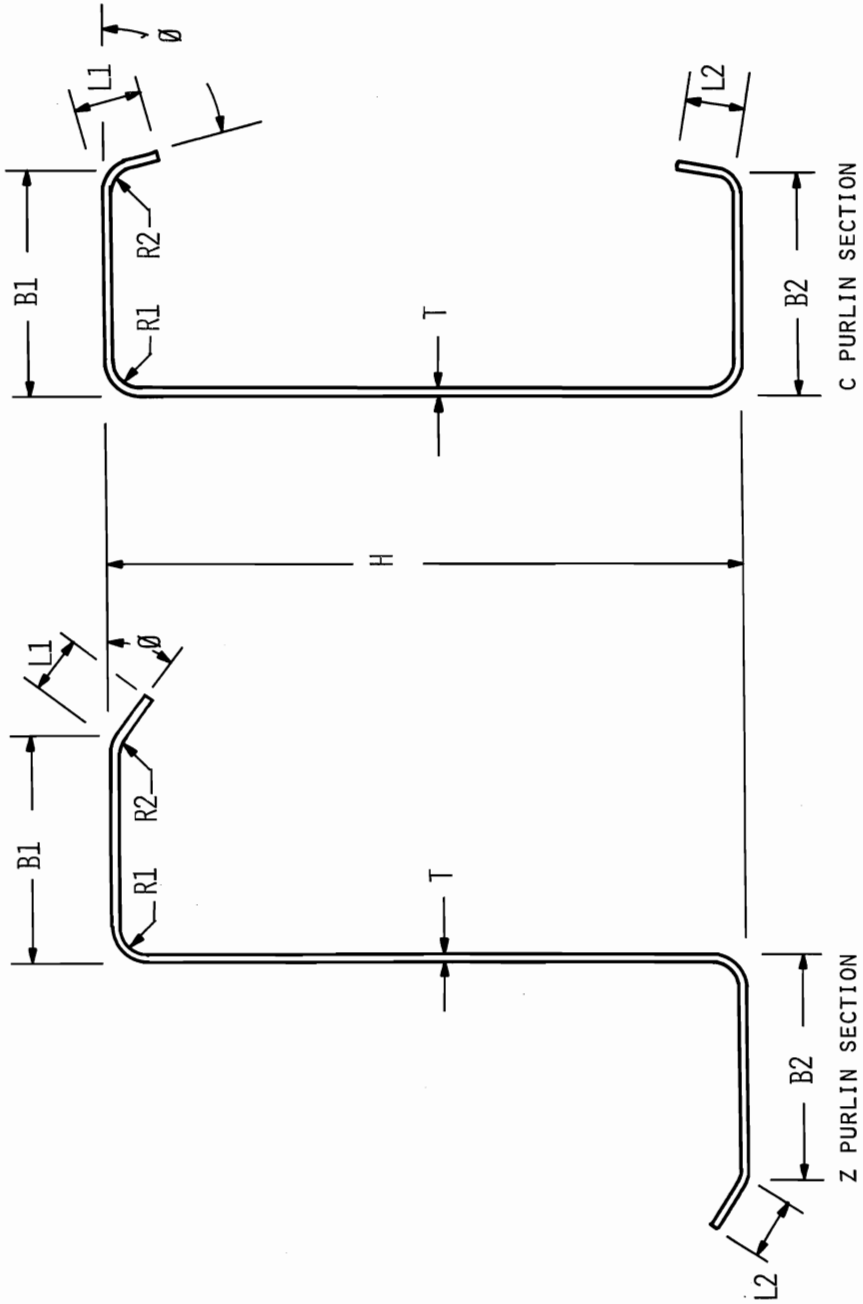


FIGURE 1 - PURLIN CROSS-SECTION

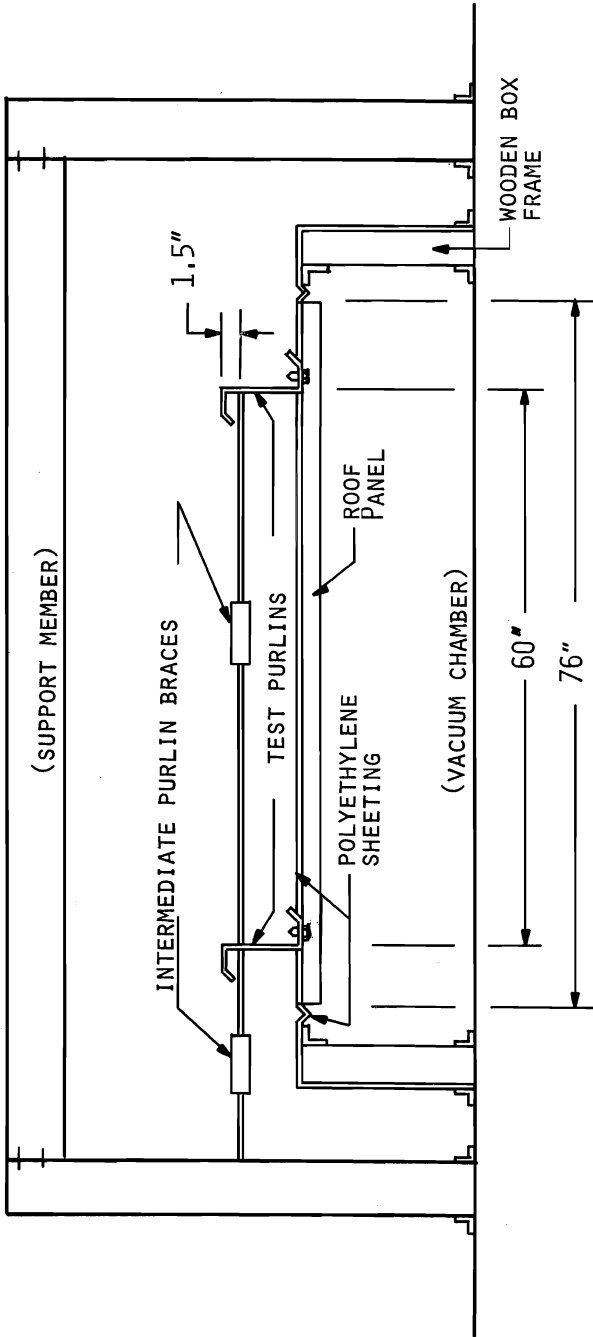


FIGURE 2 - CROSS-SECTION OF PURLIN UPLIFT VACUUM TEST CHAMBER

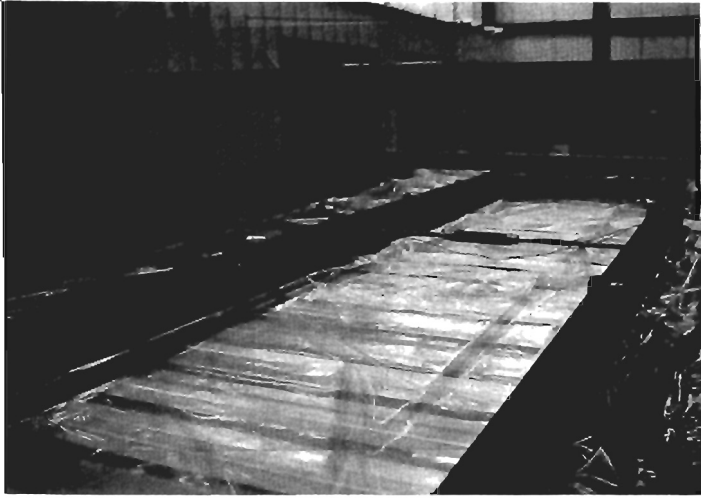


FIGURE 3 - MID-SPAN BRACE SETUP



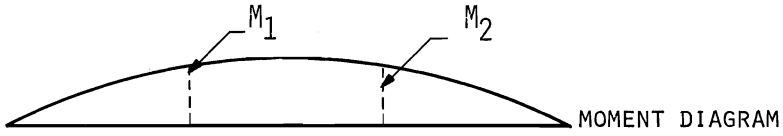
FIGURE 4 - THIRD-POINT BRACE SETUP



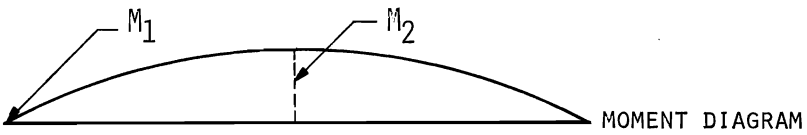
FIGURE 5 - PURLIN BRACE CONNECTION



FIGURE 6 - SCREWJACK AND SUPPORT CONNECTION



(A) BRACE AT THIRD POINT, $C_B = 1.0$



(B) BRACE AT MID-SPAN, $C_B = 1.75$

FIGURE 7 - DISTRIBUTION OF MOMENTS ALONG THE UNBRACED LENGTH